JOURNAL OF SOLID STATE CHEMISTRY 109, 35–42 (1994)

A Novel Autoignited Combustion Process for the Synthesis of Bi–Pb–Sr–Ca–Cu–O Superconductors with a T_c (0) of 125 K

P. Sujatha Devi and H. S. Maiti

Electroceramics Laboratory, Central Glass & Ceramic Research Institute, Calcutta, 700 032, India

Received December 29, 1992; in revised form June 3, 1993; accepted June 7, 1993

Zero resistivity at 125 K has been observed for the first time in bismuth system with the nominal composition $Bi_{1.75}Pb_{0.25}Sr_2Ca_2Cu_3O_{10+\delta}$ by applying a novel autoignited combustion process. The thermal decomposition characteristics of the gel and the sequence of formation of the superconducting phases are described. This combustion process is very simple, convenient, and nonexplosive, as well as economical for large scale production, of fine powder samples with higher degree of homogeneity, excellent sinterability, and reproducibility. The low T_c and the high T_c phases started forming at temperatures as low as 750 and 800°C, respectively. Powders formed have an average agglomerate size of around 0.8 μm.

INTRODUCTION

Since the discovery of the bismuth oxide superconductors by Maeda *et al.*and others (1–4) with critical transition temperatures (T_c) at about 20 K for $Bi_2Sr_2CuO_{6+\delta}$ (2201), 80 K for $Bi_2Sr_2CaCu_2O_{8+\delta}$ (2212) and 110 K for $Bi_2Sr_2Ca_2Cu_3O_{10+\delta}$ (2223), known as the so called "Polytypoids," extensive research has been carried out to stabilize or isolate these three different phases. Particularly, the highest transition temperature of the 2223 phase has encouraged researchers to focus their attention on how to stabilize or increase the volume fraction of this phase to enhance the critical temperature of the samples. There have been a number of successful attempts in many laboratories in this regard (5–9). The general conclusion that emerges from these studies is that Pb substitution enhances the relative proportion of 2223 phase in comparison to that of the low T_c 2212 phase. Nevertheless, there has been only limited success so far in synthesizing the single phase bulk samples of 2223 phase with $T_c > 110$ K, although there have been a few studies on the effect of Sb addition to the bismuth system suggesting that the T_c can be raised to as high as 140 K (10–14). A similar result of T_c enhancement has also been observed by Sastry *et al.* (15) but their sample was of a multiphasic nature. Without antimony, Wilhelm and Eibl (16) detected a transition with $T_c = 114$ K and Takada *et al.*(17) detected a phase with $T_c = 117$ K in the Bi–Pb–Sr–Ca–Cu–O system. Further, Dissanayake *et al.* (18) succeeded in getting T_c at 120 K in the bismuth system by subjecting the pellet samples to an extra annealing schedule. Hence it is apparent that the true T_c of 2223 phase can be enhanced to as high as 140 K and the values very often quoted do not represent the optimum value.

High T_c ceramic superconductors are normally prepared by the solid state reaction of mixtures of oxides and carbonates at a high temperature. With the aim of avoiding the disadvantages associated with the classical ceramic preparation method, several research groups have developed various chemical routes such as the sol–gel process (19–22), coprecipitation method (23), spray-pyrolysis (24), precursor matrix method (15, 25), citrate gel process (26–30), and combustion processes (31–33) for this purpose. The citrate gel process comparatively is found to be highly promising and was originally developed to obtain complex oxides and later on for getting perovskite oxides, spinels (34–37) and high T_c superconducting oxides (38–40).

A modified citrate process termed as the "autoignited citrate gel process" was earlier developed in our laboratory, for the preparation of YBCO superconductor (41). In this investigation the process is further improved and applied to bismuth superconductors. Briefly, this process involves a low-temperature initiated combustion process, which makes use of the heat energy liberated by the exothermic anionic oxidation reduction reaction between the citrate and nitrate ions. This combustion reaction undergoes a self-propagating and nonexplosive process, which is safe and instantaneous compared to other combustion processes (31–33). Also, this process is rapid and simple compared to the sluggish amorphous citrate process, which requires extensive thermal treatment. Moreover, this method produces materials with low levels of residual carbon and, hence, is attractive for getting compositionally homogeneous powders with large surface areas.

The present work is also aimed at studying the thermal decomposition behavior of the precursor materials as well

0022-4596/94 $6.00

as the reaction mechanisms of Pb-containing bismuth systems before and after thermal treatment by TGA, DTA, IR, XRD, etc.

EXPERIMENTAL

Powder Preparation

All chemicals used were of a high purity grade. Stock solutions of metallic nitrates in the desired proportions were mixed with an aqueous solution of citric acid. The metallic solutions were mixed in the ratio Bi : Pb : Sr : Ca : Cu = 1.75 : 0.25 : 2 : 2 : 3. One gram mole of citric acid was used for each gram mole of metal ions. Here the ratio of citrate to nitrate was fixed around 0.45. Ethylenediamine was added dropwise into the solution with constant stirring until the pH reached 6. Ethylenediamine served two principal purposes: it acts as an additional fuel for controlling the combustion process and also as an efficient complexant to prevent inhomogeneous precipitation of individual components prior to combustion. The mixed solution was stirred magnetically in a hot plate maintained at a temperature of 80–90°C. The stirring was stopped when the liquid turned viscous, but the heating was continued. The viscous liquid began to set into a gel with color change from blue to light blue and finally to green. During the formation of the gel the temperature of the system increased slowly and reached around 130°C. On further heating the green gel started to foam, and swell and when the temperature reached around 170°C, the dry gel caught fire on its own with the appearance of glowing flints and evolution of a large amount of gases. This self-sustaining spontaneous combustion process was completed within a few seconds producing brownish yellow ash. The powder ash consisted of very light and homogeneous flakes with very small particle size. It was interesting to note that unlike other combustion processes (31–33), the autocatalytic combustion occurred in this case irrespective of the heating rate, stoichiometry, and mass to volume ratio of the combustion mixture. Moreover, since this process is nonexplosive, extra caution was not necessary to avoid vigor of the reaction.

Characterization of the Products of Reaction

Thermogravimetric analysis (TGA) and differential thermal analysis (DTA) were carried out in a Shimadzu TG 50 and DTA 50 unit, at a heating rate of 10°C min^{-1} in static air and flowing argon atmospheres, to understand the pyrolysis of the precursor material. IR spectra were used to identify the intermediates formed during pyrolysis and were recorded on a Jasco 700 spectrometer with KBr pellets. The identification of various phases formed during calcination and sintering were carried out using X-ray diffraction analysis in the range 5 to 50° (2θ) in a Phillips

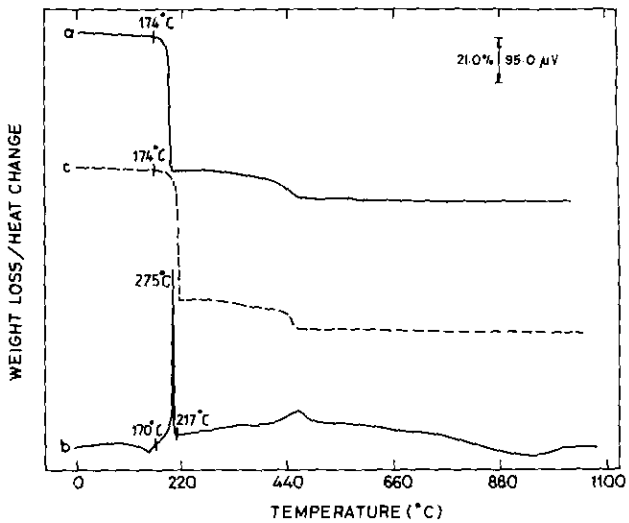

FIG. 1. (a) TG of the gel in static air, (b) DTA of the gel in static air and (c) TG of the gel in flowing argon.

diffractometer (PW 1730) with Cu$K\alpha$ radiation. Particle size analysis was done in a Micromeritics Sedigraph 5100 unit.

Pellets of the 2223 phase for resistivity measurements were obtained by sintering the pressed powders at 845°C for various timings employing a heating and a cooling rate of 100°C hr^{-1}. The temperature dependence of the electrical resistance of the sintered specimen was measured by the standard four-probe method, using air drying silver paint for the electrical contacts. Kiethley Nanovoltmeter and programable power supply were used for the purpose. The specimens were cooled inside an Oxford Instrument Model CN 1710 liquid nitrogen cryostat fitted with an ITC 4 programable temperature controller. The fracture surface of the sintered specimen was observed using a Stereoscan 250 scanning electron microscope performing at 20 kV.

RESULTS AND DISCUSSION

Thermal Characterization of the Gel and the Ash

Figures 1a–1c show the thermograms of the green gel collected prior to combustion. Figures 2a and 2b depict the thermal changes of the ash powder collected after the autocombustion process. An interesting feature of the TG curve in Fig. 1a is an almost single step decomposition behavior of the gel which starts at a temperature of 174°C. This is in contrast to a multistep decomposition behavior normally observed for the citrate gels (31, 35, 38, 39). This single step decomposition behavior associated with a very sharp and intense exotherm (Fig. 1b) is a clear indication of an autoignited combustion process. This au-

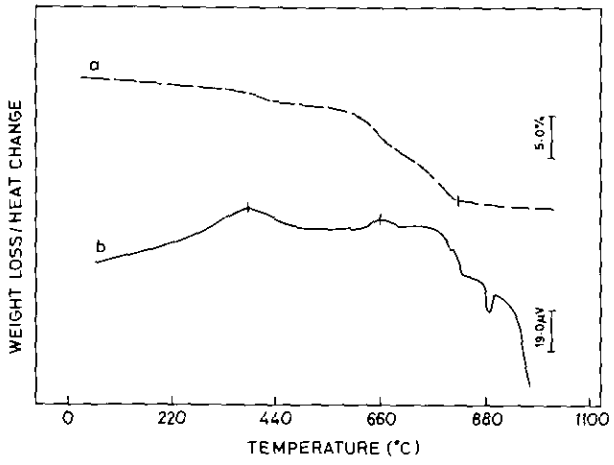

FIG. 2. (a) TG and (b) DTA of the ash powder in air.

tocombustion arises from a highly exothermic anionic oxidation reduction reaction between citrate and nitrate ions, the rate of which is controlled by the presence of ethylenediamine. As also evident from DTA the onset of this combustion process starts around 174°C and as a result of this combustion process the temperature of the system as a whole increases to 275°C as shown by DTA peak temperature. Once the combustion process is over, the temperature comes down quickly to the normal condition (217°C as noted on the DTA curve). This type of an autocatalytic combustion reaction between citrates and nitrates is observed for the first time in these systems. A similar kind of autocatalytic combustion has been observed earlier in a few other systems of this kind (41, 42). Further, TG of the gel in flowing argon atmosphere shows that (Fig. 1c) irrespective of the oxygen partial pressure the autocatalytic combustion occurs, which further supports this oxidation–reduction reaction.

Figure 1 also indicates that in addition to the autoignition step, a relatively small second decomposition step occurs at around 440°C associated with a broad exotherm. The decomposition of the gel appears to be complete within 600°C.

TGA curve of the ash after auto ignition (Fig. 2a) clearly shows that there is practically no carboxylate moiety left in the ash as the weight remains almost constant up to 350°C. The weight loss observed in the region 500–780°C is related with the elimination of residual carbonates. The corresponding DTA curve also shows two exotherms around 385 and 660°C respectively. The exotherm around 660°C might be due to carbonate decomposition together with the formation of the complex oxide phases. Other endotherms at 813, 837, and 890°C represents crystallization and melting of these phases. Comparison of the Figs 1 and 2 indicate that when the dried gel is heated slowly inside a thermal analyzer, it decomposes into a constant weight within 600°C. On the other hand when the gel is allowed to burn on its own on a hot plate the ash contains small amounts of residual carbonates which takes slightly higher temperature (up to 780°C) for their complete removal.

Physical Characterization of Ash and Calcined Powders

Figures 3a–3e represents the IR spectra of the gel, ash, and its various calcination products. The spectrum of the "as dried" gel (curve a) shows peaks with characteristic frequencies of ionic nitrates and carboxylate ions. The spectrum of the ash sample (curve b) shows the typical carbonate vibrations at ~1473 cm^{-1} (triply degenerated stretching mode V_3), ~875–860 cm^{-1} (doubly degenerated stretching mode ~V_2) and 710 cm^{-1} (triply degenerated bending mode V_4) respectively, and also a broad band below 700 cm^{-1} assigned to metalloxane bands. IR spectrum of the 600°C calcined sample (curve c) also retains the fundamental vibration bands of the carbonate CO_3^{2-}. However, beyond 600°C the band intensities decrease monotonically and approach zero above 750°C (curve d). A spectrum of the 800°C calcined sample does not reveal the presence of any carbonate indicating clearly the complete decomposition of the carbonate at this stage. The observed IR bands indicating the presence of carbonates as intermediates is in accordance with what has been reported very recently by Lee *et al.* (43).

The results of phase identification for the ignited ash and the calcined powders by X-ray diffraction analysis are shown in Fig. 4. The ignited ash is already a mixture of reactive oxides and carbonates with trace amounts of the 2201 phase. The XRD pattern of the ash obtained in this investigation is almost identical to that of the powder calcined at 600°C in a sol–gel process reported earlier (18), which indicates that calcination steps up to 600°C

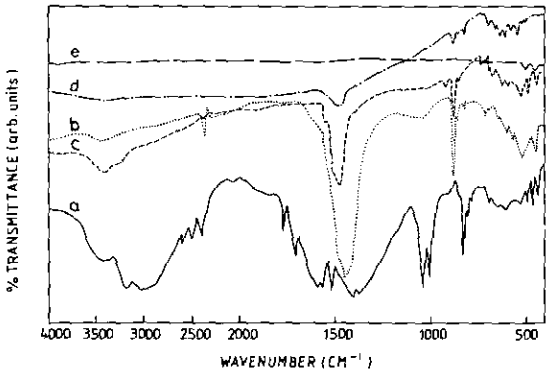

FIG. 3. The IR spectra of (a) as dried gel, (b) ash after autoignition (c) ash calcined at 600°C/4 hr (d) ash calcined at 750°C/4 hr, and (e) ash calcined at 800°C/4 hr.

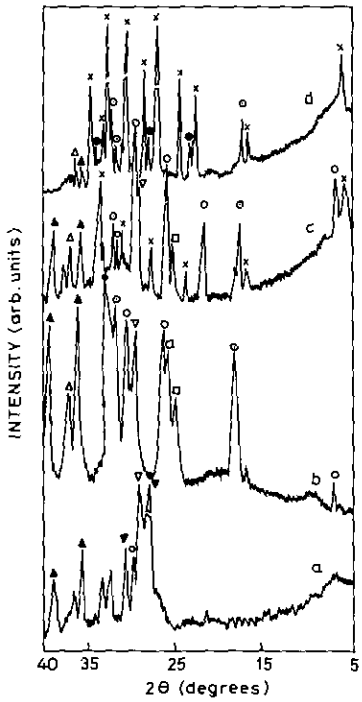

FIG. 4. X-ray diffraction patterns of ash (a) after autoignition, (b) calcined at 600°C/4 hr, (c) calcined at 750°C/4 hr, and (d) calcined at 800°C/4 hr. ● 2223, × 2212, ○ 2201, ⊙ Ca_2PbO_4, ▲ CuO, △ Ca_2CuO_3, ◀ Bi_2O_3, ◁ $CaCO_3$, □ $SrCO_3$.

can be avoided in this case. When the ash sample was fired up to 600°C for 4 hr, Ca_2PbO_4, Ca_2CuO_3, CuO, and $Bi_2Sr_2CuO_{6+\delta}$ (2201) were detected as the major phases (Fig. 4b). 2201 was found to be the major phase in the 750°C/4 hr calcined sample with small amounts of 2212 as the secondary phase (Fig. 4c). As the sample was calcined at 800°C/4 hr, 2201 decayed completely resulting in the formation of $Bi_2Sr_2CaCu_2O_{8+\delta}$ as the major phase with small amounts of $Bi_2Sr_2Ca_2Cu_3O_{10+\delta}$ (2223) phase (Fig. 4d). The low T_c phase (2212) may be produced by the reaction of 2201 phase with Ca_2CuO_3 and copper oxide (since they have shown a reduction in intensity). The significant point here is that the high T_c phase has started forming as early as 800°/4 hr, although the intensity is much less. This temperature is remarkably lower than that has been reported earlier for the initiation of the phase formation (13, 14, 18, 19). Moreover from the XRD patterns presented later in Fig. 9a, it is clear that the 2223 phase formation is more or less complete by 48 hr of sintering at 845°C. Beyond 850°C, 2223 phase decomposes further to form 2212 and thereby decreasing the volume fraction of the 2223 phase. The further the temperature deviates upwards from 845°C the less is the volume fraction of the 2223 phase present.

Figure 5 depicts the results of DTA of the powders calcined at various temperatures. Figure 5a represents the DTA of the powder calcined at 600°C. The broad exotherm around 730°C might represent the decomposition of carbonates followed by some reactions leading to phase formation/crystallization. The small endotherm at 825°C represents the melting of Ca_2PbO_4. The endotherm at 895°C is attributed to the melting of 2201 phase. The endotherm at 960°C might be due to melting reaction of residual materials (37). The DTA of the 750°C calcined powder (Fig. 5b) also shows endotherm at 895°C indicating the melting of 2201 phase and thereby indicating the presence of 2201 as the major phase. For the 800°C calcined sample the onset of melting starts around 853°C and this lower melting point clearly indicates the presence or incorporation of Pb into the lattice. It also indicates that beyond 890°C the phase is unstable and it decomposes to other higher melting phases. For the sample sintered at 845°C for 120 hr (which is found to be the homogeneous 2223 phase), the onset of melting starts around 850°C and beyond 870°C, it decomposes and forms other high melting phases as evident from the DTA. The observed melting temperatures are in accordance with the previously recorded values (19, 44–47). The experimental results clearly indicate that the phases identified by XRD are in accordance with those determined by IR and also corroborate the DTA results. Thus it is evident that the high T_c phase is produced through the lwo T_c phase which was formed as an intermediate reaction product and also as a precursor of the high T_c phase.

Based on the observed experimental results a tentative reaction path for the formation of the Pb doped 2223 phase including the possible intermediate phase formations may be proposed as follows:

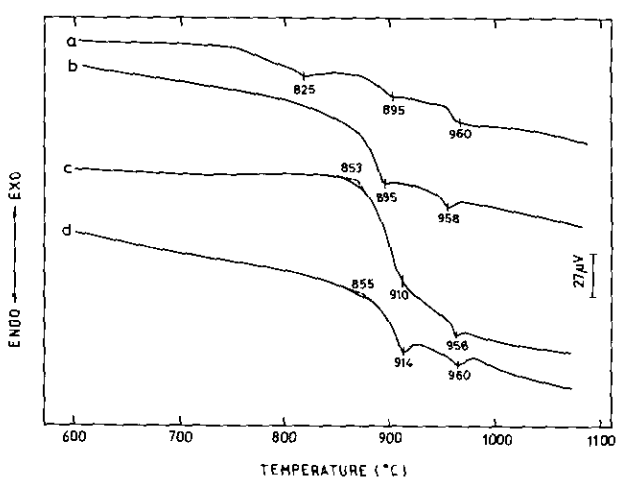

FIG. 5. The DTA of the various calcined and sintered products (a) 600°C/4 hr, (b) 750°C/4 hr, (c) 800°C/4 hr, and (d) 845°C/120 hr.

Precursor gel

↓ Autoignition ~170°C

$Bi_2O_3 + CuO + CaCO_3 + Bi_2Sr_2CuO_{6+\delta}$ (ash)

↓ ≤600°C

$Ca_2PbO_4 + CaCO_3 + SrCO_3 + CuO + Ca_2CuO_3 + Bi_2Sr_2CuO_{6+\delta}$

↓ 600–750°C

$Ca_2PbO_4 + CuO + Ca_2CuO_3 + Bi_2Sr_2CuO_{6+\delta}$

↓ 750–800°C

$Bi_2Sr_2CaCu_2O_{8+\delta} + Ca_2PbO_4 + CuO + Ca_2CuO_3$

↓ 800–840°C

$Bi_{1.75}Pb_{0.25}Sr_2Ca_2Cu_3O_{10+\delta} + Bi_2Sr_2CaCu_2O_{8+\delta}$ (trace)

↓ 845–850°C

$Bi_{1.75}Pb_{0.25}Sr_2Ca_2Cu_3O_{10+\delta}$

2212 phase is formed by the reaction between 2201 phase with Ca_2CuO_3 and CuO. The formation of Ca_2PbO_4 phase at a low temperature makes it possible to decompose the carbonates at low temperature. Above 820°C Ca_2PbO_4 melts, which may play the role of a catalyst/flux to fuse 2212, CuO, and residual Ca_2CuO_3 and thus leading to the formation of 2223 phase. The melting of the Ca_2PbO_4 facilitates the dissolution of CuO and Ca_2CuO_3 and provides a pathway for the diffusion of Ca^{2+} and Cu^{2+} to the reaction site. Therefore, the formation and melting of the intermediate phase Ca_2PbO_4 at relatively lower temperatures (40, 47) are the two key steps for the preferred formation of a single 2223 phase. Our assumption is also in agreement with other reports where the role of Ca_2PbO_4 in the formation of the high T_c phase have been suggested (47–50). The transformation of the low T_c phase into the high T_c phase essentially involves the thermally activated long range diffusion of the various constituents as indicated above. It has been found that partial substitution of lead for bismuth in BiO layers can create vacancies in oxygen sites (18) or alters the defect structure (50) which may reduce the energy barrier for the insertion of Ca and CuO_2 layers into 2201 to form 2212 or into 2212 to form the 2223 phase. Since such insertions are kinetically very slow processes, heat treatment time need to be prolonged considerably for the complete formation of the 2223 phase irrespective of the preparation conditions. It is noteworthy that in this method developed by us, the temperature and time necessary to get the desired superconducting phase is remarkably lower than the precursor matrix method or other conventional methods (15, 21, 25, 50–53). In this connection it may be mentioned that Zhu and Nicholson (54) who adopted the method of decomposition of nitrates, reported complete formation of 2223 phase by

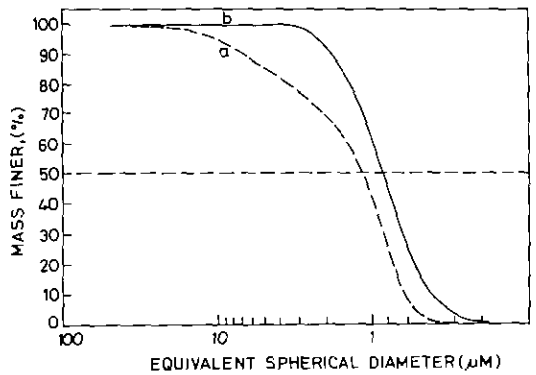

FIG. 6. The particle size distribution of the powder calcined at 800°C/4 hr.

sintering the pellets at 845–865°C for 12 to 36 hr. However, they used intermediate grinding and repressing between repeated sintering in addition to maintaining low oxygen partial pressure. They also used a prolonged calcination (48 hr) at 800°C. In our autocombustion process initial calcination is done for a very short period (800°C/4 hr) during which the phase formation starts and is completed at a sintering temperature of 845°C within a period of 48 hr, without any intermediate grinding and pressing or use of reduced oxygen partial pressure. Our DTA and XRD results also indicate that the range of sintering temperature within which the 2223 phase remains stable is rather limited and the optimum temperature for the preferred growth of the 2223 phase is between 845–855°C.

Figure 6 indicates the particle size distribution of the powder calcined at 800°C for 4 hr. The graph indicates a mean agglomerate size of ~1 μm. On wet milling in the planetary mill with butanol reduces the average particle size to 0.8 μm (Fig. 6b). Hence the agglomerates appear to be weakly bonded and it is anticipated that they will be broken down during the subsequent powder compaction process. However the surface morphology of this powder also indicates appreciable particle agglomeration (Fig. 7a). The agglomerate size of ~1 μm suggest that the finer particles have a strong tendency to cluster into weakly bonded agglomerates through a small degree of ceramic bonding (55).

Electrical and Microstructural Characterization of Sintered Specimens

Figure 8 demonstrates the characteristic temperature dependence of electrical resistance of $Bi_{1.75}Pb_{0.75}Sr_2Ca_2Cu_3O_{10+\delta}$ bulk specimens sintered at 845°C for different lengths of time viz. 48, 96, and 120 hr. Even though the potential drop for the curve a decreased significantly with lowering of temperature, zero resistance could not be observed down to 77 K, the lowest temperature limit for our experiments. Curve b also show nearly similar behav-

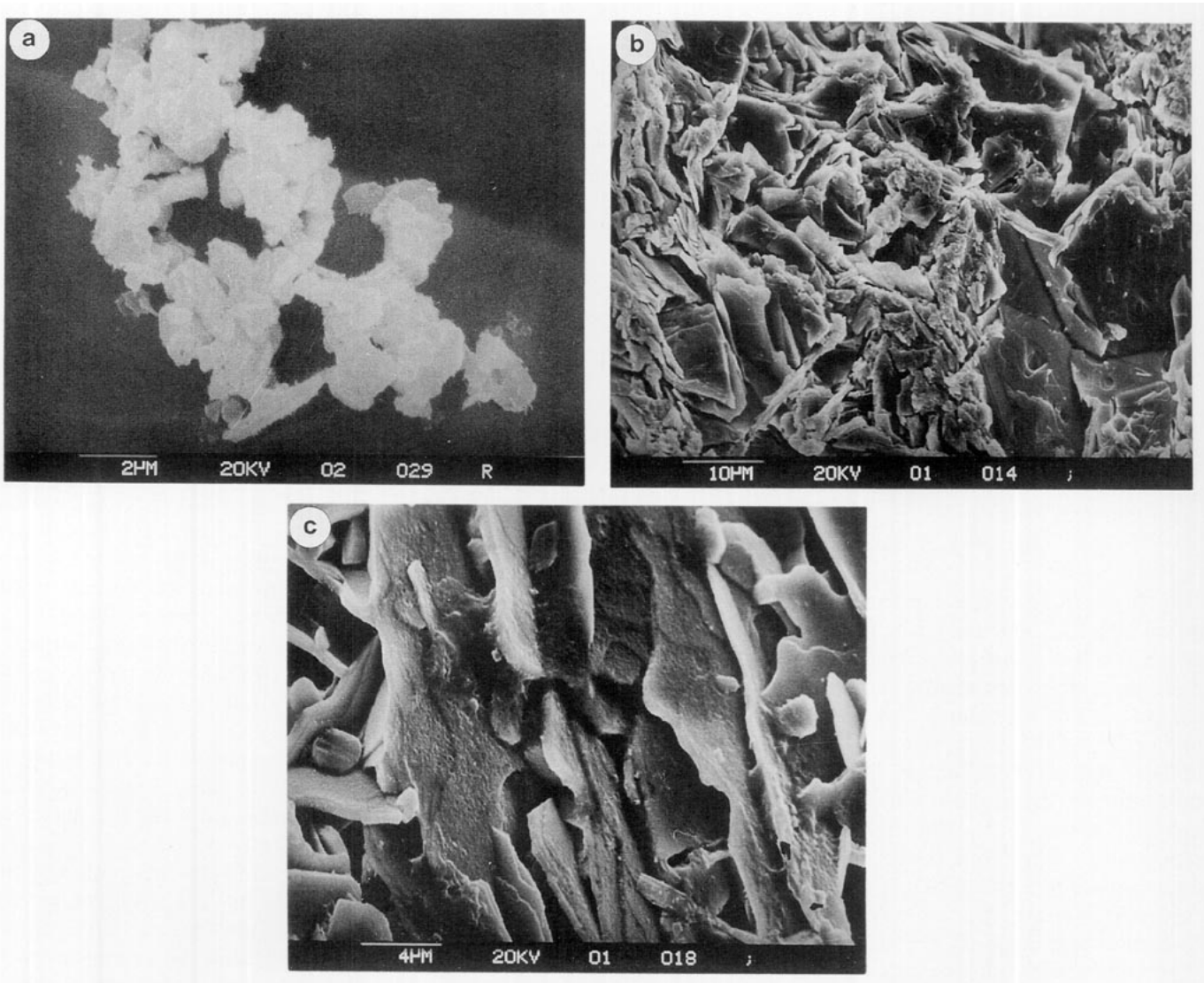

FIG. 7. Scanning electron micrograph of (a) calcined powder showing particle agglomeration, (b) fracture surface of 2223 pellets showing lamellar feature of the grains, and (c) a few oriented grains.

ior except that the voltage drop around 100 K is little more sharp. This sample also does not show zero resistance above 77 K. Since the XRDs of both these samples confirm (Fig. 9) that they are phase pure, it suggests that the superconducting coupling between grains is still very weak. However, the sample corresponding to curve c which is sintered at 845°C for 120 hr showed a sharp T_c onset at 140 K and T_c (0) at 125 K. These observations supports the mechanism that the treatment by prolonging the sintering time is more effective in stabilizing the 2223 phase and consequently increasing the T_c value. The more likely explanation for this very high T_c onset and T_c (0) is that the powders prepared by this process has excellent homogeneity and sinterability. It may be pointed out here that without any extra thermal annealing cycle, repressing or heat treatment conditions (11–16, 55–57), zero resistivity at 125 K has been achieved for the first time in this investigation for the $Bi_{1.75}Pb_{0.25}Sr_2Ca_2Cu_3O_{10+\delta}$ system. It is also interesting to note that this sample shows another sharp resistivity drop at a temperature as high as 250 K. However, we have not made any systematic attempt to understand this behavior.

The sample was given three cycles of cooling to liquid nitrogen and heating back to room temperature and the T_c (0) still remained as 125 K. Moreover, after 30 days of exposure of the sample to the ambient atmosphere the T_c (0) was observed to be constant. Hence no aging effect was observed in our specimens. The bulk pellet showed a critical current density of 96 $A \cdot cm^{-2}$.

Figures 7b and 7c illustrate the fracture surface of the sample sintered at 845°C for 120 h. The micrograph apparently shows that the sample is composed of lamellar plate

like grains which seem at first glance to be irregularly oriented. At higher magnifications it shows that the grains are oriented. Moreover, it is clear that there is no secondary phase at the grain boundaries which deteriorates the superconducting transition. Also the grains are fairly large enough with an average grain size of around 15–20 μm and these plate-like elongated grains have a tendency to align parallel to each other and hence can form well connected grains. Thus the improvement in superconducting characteristics of this sample seems to be influenced also by the increased coupling among grains, which in turn is associated with the high sinterability of the autoignited precursor material.

XRD patterns of variously sintered specimen are shown in Fig. 9. Since the (001) lines of the high T_c phase are a little stronger than the others, it may be concluded that the grains are oriented in the direction of c-axis. The XRD patterns of the sample also indicate that the relative intensity of various reflections has varied slightly, as the 2223 phase grows at the expense of the 2212 phase. A similar change in the X-ray intensity has been reported earlier for the bismuth systems with T_c's above 120 K (11, 18). The tetragonal lattice constants were refined by the least square method and the results were found to be as $a = 5.414$ Å and $c = 37.50$ Å respectively. In comparison to the reported values for 2223 singlephase (58, 59) the c-axis here is longer by 0.4 Å. This elongation is quite remarkable and is believed to be the major factor responsible for the observed enhancement in T_c. This argument is further strengthened from the observation of Takada *et al.* (17) and Wilhelm and Eibl (16) where T_c enhancement to the extent of 117 K has been assigned to c-axis elongation. Hence, it is assumed that some subtle structural change occurs in the system, with elongation of c-axis when there is an appreciable enhancement in T_c.

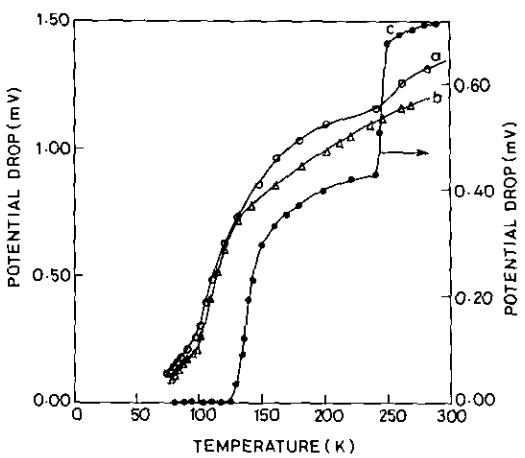

FIG. 8. *Temperature dependence of potential drop (for a constant current) across the specimens sintered at 845°C for various times (a) 48 hr, (b) 96 hr, and (c) 120 hr.*

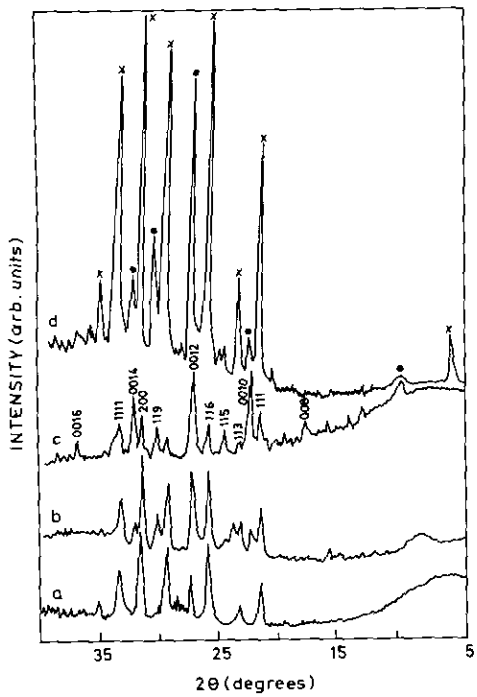

FIG. 9. X-ray diffraction patterns of the specimens sintered at (a) 845°C/48 hr, (b) 845°C/96 hr, (c) 845°C/120 hr, and (d) 860°C/40 hr. × 2212, ● 2223.

Furthermore the volume fraction of our high T_c Phase is estimated to be more than 95% considering the detection limit of the X-ray diffraction. Apart from these the strong coupling between the grains and high homogeneity of the powder as revealed from X-ray and chemical analysis also would favor an enhancement in T_c in these systems.

CONCLUSION

The autoignition of citrate gel is a very simple and convenient route to obtain fine powder samples of bismuth superconductors with higher degree of homogeneity as well as reproducibility with a very low level of undesired phases. This combustion process appears to undergo a self-propagating and nonexplosive exothermic reaction. We have investigated the materials chemistry involved in the formation of high T_c bismuth superconductor by using the techniques like TG, DTA, IR, XRD, etc. Thermogravimetric analysis of the gel revealed an almost single step decomposition process, giving a clear evidence for an autoignited combustion process. Zero resistivity at 125 K has been observed for the first time in bismuth systems by applying this autoignition process. The optimum temperature for the formation of the 2223 phase is around 850 ± 5°C. It is expected that the use of this technique would provide avenues to synthesize new superconducting compounds as is evident from our interesting results.

ACKNOWLEDGMENTS

Authors are grateful to the Director of CGCRI for his kind permission to publish this work. One of the authors (P. S. D.) gratefully acknowledges the financial support by CSIR, government of India. The authors are thankful to Mr. Asim Halder, Dr. S. N. Roy, and Mr. D. Bhattacharya for their help and cooperation.

REFERENCES

1. H. Maeda, Y. Tanaka, M. Fukutomi, and T. Asano, *Jpn. J. Appl. Phys.* **27,** 209 (1988).
2. C. Michel, M. Hervieu, M. M. Borel, A. Grandin, F. Deslandes, J. Provost, and B. Raveau, *Z. Phys. B Condes. Matter* **68,** 421 (1987).
3. R. M. Hazen, C. T. Prewitt, R. J. Angel, N. L. Ross, L. W. Finger, C. G. Hadidiacos, D. R. Veblen, P. J. Heaney, P. H. Hor, R. L. Meng, Y. Y. Sun, Y. Q. Wang, Y. Y. Xue, Z. J. Huang, L. Gao, J. Bechtold, and C. W. Chu, *Phys. Rev. Lett.* **60,** 1174 (1988).
4. J. M. Tarascon, Y. Le Page, L. H. Greene, B. G. Bagley, P. Barboux, D. M. Hwang, G. W. Hull, W. R. McKinnon, and M. Giroud. *Phys. Rev. B* **38,** 2504 (1988).
5. M. Takano, J. Takada, K. Oda, H. Kitaguchi, Y. Miura, Y, Ikeda, Y. Tomii, and H. Mazaki, *Jpn. J. Appl. Phys.* **27,** L1041 (1988).
6. T. Toshihisa, Y. Tanaka, M. Fukutomi, K. Jikihara, J. Machida, and H. Maeda, *Jpn. J. Appl. Phys.* **27,** 1652 (1988).
7. N. Kijima, H. Endo, J. Tsuchiya, N. Kijima, M. Mizuno, and Y. Oguri, *Jpn. J. Appl. Phys.* **27,** L821 (1988).
8. H. Nobumasa, K. Shimizu, Y. Kitano, and T. Kawai, *Jpn. J. Appl. Phys.* **27,** L846 (1988).
9. T. Komatsu, R. Sato, C. Hirose, K. Matusita, and T. Yamashita, *Jpn. J. Appl. Phys.* **27,** L2293 (1988).
10. L. Hongbao, C. Liezhao, Z. Ling, M. Zhigiant, I. Xiaoxian, Y. Zhidong, X. Bai, M. Xiang, Z. Guien, R. Yaozhaog, C. Zhaojia, and Z. Yuheng, *Solid. State Commun.* **69,** 867 (1989).
11. M. R. Chandrachood, I. S. Mulla, and A. P. B. Sinha, *Appl. Phys. Lett.* **55,** 1472 (1989).
12. H. Liu, L. Cao, L. Zhao, Z. Mao, X. Li, Z. Yu, B. Xue, G. Zhou, Y. Run, Z. Chen, and Y. Zhang, *Solid State Commun.* **69,** 867 (1989).
13. K. Fischer, A. Rojek, S. Thierfeldt, H. Lippert, and R. R. Arons, *Physica C* **160,** 466 (1989).
14. J. A. A. Khan, N. M. Butt, A. Mahmood, R. Shaheen, G. Bashir, and K. A. Shahid, *J. Mater. Sci.* **27,** 6321 (1992).
15. P. V. P. S. S. Sastry, I. K. Gopalakrishnan, J. B. Yakhmi, and R. M. Iyer, *Physica C* **157,** 491 (1988).
16. M. Wilhelm and O. Eibl, *Solid State Commun.* **70,** 137 (1989).
17. J. Takada, H. Kitaguchi, T. Egi, K. Oda, Y. Miura, H. Mazaki, Y. Ikeda, Z. Hiroi, M. Takano, and Y. Tomii, *Physica C* **170,** 249 (1990).
18. M. A. K. L. Dissanayake, M. J. S. J. Sooriyajeewan, S. H. S. P. Samarappuli, N. D. Karunasingha, and B. G. S. Samarawickrama, *Mater. Lett.* **12,** 403 (1992).
19. Y. Masuda, R. Ogawa, Y. Kawate, T. Taeishi, and N. Hara, *J. Mater. Res.* **7,** 292 (1992).
20. H. R. Zhuang, H. Kozuka, and S. Sakka, *J. Mater. Sci.* **25,** 4762 (1990).
21. A. Nozue, H. Nasu, K. Kamiya, and K. Tanaka, *J. Mater. Sci.* **26,** 4427 (1991).
22. F. H. Chen, H. S. Koo, and T. Y. Tseng, *J. Mater. Sci.* **25,** 3338 (1990).
23. C. Y. Shei, R. S. Liu, C. T. Chang, and P. T. Wu, *Inorg. Chem.* **29,** 3117 (1990).
24. N. Tohge, M. Tatsumisago, T. Minami, K. Okuyama, K. Arai, and Y. Kousaka, *Jpn. J. Appl. Phys.* **28,** L1175 (1989).
25. Z. Wang, B. W. Statt, M. J. G. Lee, S. Bagheri, and J. Rutter, *J. Mater. Res.* **6,** 1160 (1991).
26. T. S. Heh, J. R. Chen, and T. Y. Tseng, *Jpn. J. Appl. Phys.* **29,** 652 (1990).
27. N. H. Wang, C. M. Wang, H. C. I. Kao, D. C. Ling, H. C. Ku, and K. H. Lu, *Jpn. J. Appl. Phys.* **28,** L1505 (1989).
28. R. S. Liu, W. N. Wang, C. T. Chang, and P. T. Wu, *Jpn. J. Appl. Phys.* **28,** L2155 (1989).
29. A. Aoki, *Jpn. J. Appl. Phys.* **29,** L270 (1990).
30. F. R. Sale and F. Mahloojchi, *Ceram. Int.* **14,** 229 (1988).
31. D. Rambabu, *Jpn. J. Appl. Phys.* **29,** L507 (1990).
32. L. R. Pederson, G. D. Maupin, W. J. Weber, D. J. McReady, and R. W. Stephens, *Mater. Lett.* **10,** 437 (1990).
33. J. J. Kingsley and K. C. Patil, *Mater. Lett.* **6,** 427 (1988).
34. D. J. Anderton and F. R. Sale, *Powder Metall.* **1,** 14 (1979).
35. M. S. G. Baythoun and F. R. Sale, *J. Mater. Sci.* **17,** 2757 (1982).
36. P. Sujatha Devi and M. Subba Rao, *Thermochim. Acta* **153,** 181 (1989).
37. P. Sujatha Devi and M. Subba Rao, *J. Solid State Chem.* **98,** 237 (1992).
38. C. T. Chu and B. Dunn, *J. Am. Ceram. Soc.* **70,** C375 (1987).
39. T. M. Chen and Y. H. Hu, *J. Solid State Chem.* **97,** 124 (1992).
40. K. Ma and A. C. Pierre, *J. Mater. Res.* **7,** 1328 (1992).
41. S. Roy, A. Das Sharma, S. N. Roy, and H. S. Maiti, *J. Mater. Res.* in press.
42. K. Kourtakis, M. Robbins, and P. K. Gallagher, *J. Solid State Chem.* **83,** 230 (1989).
43. W. H. Lee, H. Hosono, and Y. Abe, *J. Am. Ceram. Soc.* **75,** 1658 (1992).
44. K. H. Yoon and H. B. Lee, *J. Mater. Sci.* **26,** 5101 (1991).
45. T. Kanai, T. Kumagai, A. Soeta, T. Suzuki, K. Aihara, T. Kamao, and S. Matsuda, *in* "Advances in Superconductivity" (K. Kitazawa and T. Ishiguro, Eds.), p. 863. Springer-Verlag, Tokyo, 1989.
46. K. Numata, K. Mori, Yamamoto, H. Sekine, K. Inone, and H. Maeda, *in* "Advances in Superconductivity" (K. Kitazawa and T. Ishiguro, Eds.), p. 885. Springer-Verlag, Tokyo, 1989.
47. Y. L. Chen and R. Stevens, *J. Am. Ceram. Soc.* **75,** 1150 (1992).
48. N. Kijima, H. Endo, J. Tsuchiya, A. Sumiyama, M. Mizuno, and Y. Oguni, *Jpn. J. Appl. Phys.* **28,** L1852 (1988).
49. T. Uzumaki, K. Yanamaka, N. Kamehara, and K. Niwa, *Jpn. J. Appl. Phys.* **28,** L75 (1989).
50. P. L. Upadhyay, S. U. M. Rao, K. C. Nagpal, and S. G. Sharma, *Mater. Res. Bull.* **27,** 109 (1992).
51. Y. L. Chen and R. Stevens, *J. Am. Ceram. Soc.* **75,** 1150 (1992).
52. T. M. Chen and Y. H. Hu, *J. Solid State Chem.* **97,** 124 (1992).
53. A. Maqsood, M. Maqsood, M. S. Awan, and N. Amin, *J. Mater. Sci.* **26,** 4893 (1991).
54. W. Zhu and P. S. Nicholson, *J. Mater. Res.* **7,** 38 (1992).
55. T. Asano, Y. Tanaka, M. Fukutomi, K. Jikihara, and H. Maeda, Jpn. *J. Appl. Phys.* **28,** L595 (1989).
56. D. A. Harrison, R. Stevens, and S. J. Milne, *J. Mater. Sci. Lett.* **6,** 673 (1987).
57. J. Takada, H. Kitaguchi, T. Egi, K. Oda, Y. Miura, H. Mazaki, Y. Ikeda, Z. Hiroi, M. Takano, and Y. Tomii, *Physica C* **170,** 249 (1990).
58. G. Calestani, C. Rizzoli, G. D. Andreetti, E. Buluggiu, D. C. Giori, A. Valenti, A. Vera, and G. Amoretti, *Physica C* **158,** 217 (1989).
59. V. Primo, F. Sapina, M. J. Sanchis, R. Ibanez, A. Beltran, and D. Beltran, *Mater. Lett.* **15,** 149 (1992).